ISSN 8755-6839

SCIENCE OF **TSUNAMI HAZARDS**

Journal of Tsunami Society International

Volume 29 **Number 2** **2010**

OPTIMAL LOCATION OF TSUNAMI WARNING BUOYS AND SEA LEVEL MONITORING STATIONS IN THE MEDITERRANEAN SEA

Layna Groen, Anthony Joseph, Eileen Black, Marianne Menictas, Winson Tam, Mathew Gabor
Department of Mathematical Sciences,
University of Technology,
PO Box 123 Broadway, Sydney, NSW
AUSTRALIA

ABSTRACT

The present study determines the optimal location of detection components of a tsunami warning system in the Mediterranean region given the existing and planned infrastructure. Specifically, we examine the locations of existing tsunameters DART buoys and coastal sea-level monitoring stations to see if additional buoys and stations will improve the proportion of the coastal population that may receive a warning ensuring a timely response. A spreadsheet model is used to examine this issue. Based on the historical record of tsunamis and assuming international cooperation in tsunami detection, it is demonstrated that the existing network of sea level stations and tsunameters enable around ninety percent of the coastal population of the Mediterranean Sea to receive a 15 minute warning. Improvement in this result can be achieved through investment in additional real-time, coastal, sea level monitoring stations. This work was undertaken as a final year undergraduate research project.

Key words: tsunami warning system, spreadsheet modelling, optimal location.

1. INTRODUCTION

The historic record documents that numerous large destructive earthquakes and tsunamis have occurred from antiquity to the present in the Mediterranean Sea. The record goes as far back as 1628 BC when an ultra-Plinian explosion of the Santorin volcano in the Aegean Sea and the subsequent collapse of its caldera generated tsunami waves that reached up to 60 meters in height. The waves generated by this explosion/collapse and subsequent flank failures of the volcano are believed to have contributed to the destruction of the Minoan empire and civilization (Pararas-Carayannis, 1973, 1974, 1992). On July 21, 365 A.D., a great earthquake with magnitude estimated at 8.3 near the west coast of the island of Crete generated a catastrophic tsunami that was responsible for extensive destruction on Crete, Peloponnese, Eastern Sicily, Cyprus, Northern Africa, Egypt and elsewhere. The historical accounts indicate that as many as 50,000 people lost their lives in Alexandria alone. The combined catastrophic impacts of the earthquake and of the tsunami, are believed to have been a significant catalyst in the declination of the Roman Empire and its subsequent division between the East and the West (Byzantine) in 395 A.D. (Pararas-Carayannis & Mader, 2010). On October 1790, a destructive earthquake occurred near Oran city in the western part of Algeria generated a tsunami that inundated the Spanish and North Africa coasts (Amir and Cisternas, 2010).

Tsunami activity in the region has continued to the present. For example, the earthquake of 17 August 1999 in Turkey generated a destructive earthquake in the Gulf of Izmit and the Marmara Sea. The combined effects of the earthquake and tsunami were responsible for about 17,000 deaths of people and thousands of injuries. (Tsunami Institute 2009). On the Western Mediterranean, a tsunami near the Algerian coast in May 2003, "destroyed over 100 boats on Mallorca and flooded Palmas Paseo Maritimo" (Tsunami Institute 2009).

The ongoing complex interactive tectonic activity raises questions about the recurrence of another great tsunamigenic earthquake and its potential impact in the Eastern Mediterranean region (Pararas-Carayannis & Mader, 2010). The University of Cambridge notes that "the fault near Crete is accumulating strain energy " and that subsequent earthquakes could result in another tsunami having a catastrophic impact on the more populated coastal cities of the Eastern Mediterranean region (University of Cambridge 2009).

Figure 1 shows the shows source regions in the Mediterranean Sea that generated destructive tsunamis, dating back to 1628BC. Apparently all coastal regions in both the Eastern and Western Mediterranean are vulnerable to tsunamis generated from distant as well as local earthquakes. However, the record indicates that the west coast of Greece and coastal areas bounding the Aegean Sea, have the highest vulnerability. In spite of the high risk, vulnerability and high probability for the generation of destructive tsunamis, no tsunami warning system exists presently in the region (Belfast Telegraph 2009; Westall, 2008), although an implementation plan has been proposed (ICG/NEAMTWS-III 2007).

The present study investigates the best configuration of existing and new tsunami warning detectors that are needed – DART buoys and sea level monitoring stations – to maximise the effectiveness of an early warning system that could alert promptly the maximum number of people in the region of an impending tsunami. The potential performance of such as system is evaluated, based on the established historical records of tsunamis in the region.

In the following sections, we first provide a brief background of the problem as well as an outline of previous work in determining the optimal locations for the placement of tsunami detectors. Subsequently, we present an approach that can be used to assess the effectiveness of the current and expanded detector placement configurations. We then describe the data and solution approach and present the results and analysis of the current and expanded configurations. Included in the analysis is a brief discussion on the sensitivity of our results to different tsunami wave travel times and response times. We conclude the paper with a discussion of our findings.

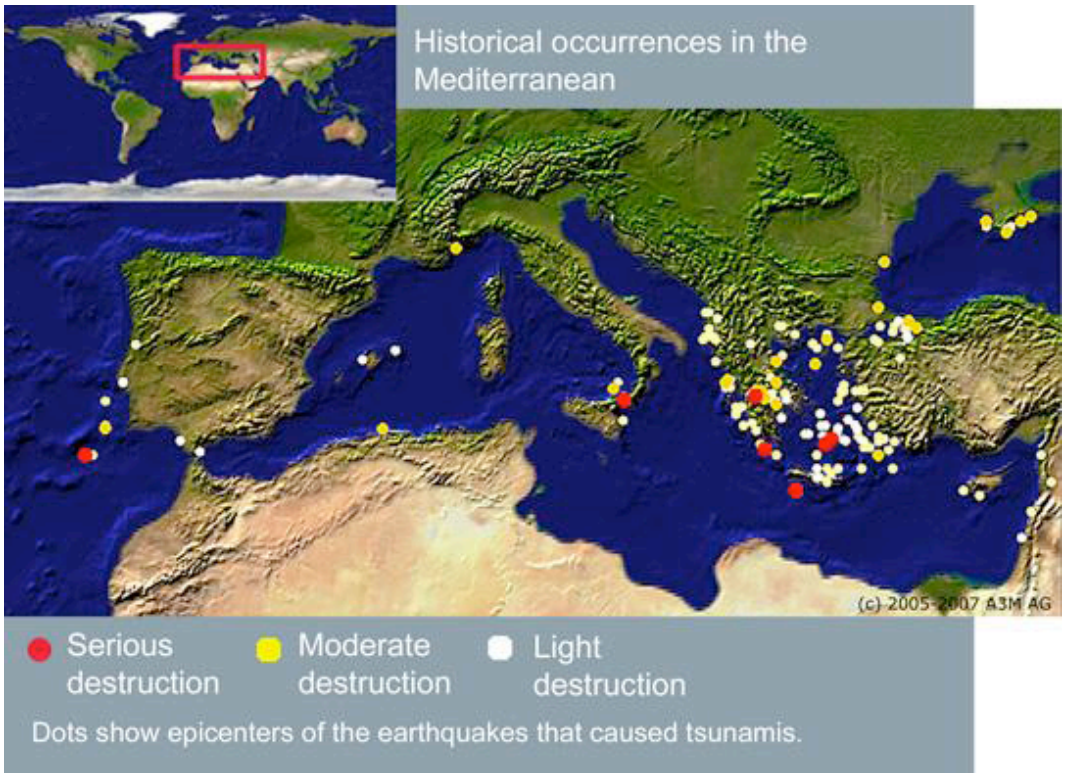

Figure 1 – Historical occurrences of Tsunamis in the Mediterranean Sea
Image Source: (Tsunami Institute 2009)

2. BACKGROUND

The seismotectonics of the Mediterranean region are dominated by the collision of Eurasia, Africa and Arabia plates and of two microplates - the Anatolian and the Aegean (Pararas-Carayannis & Mader 2010). A number of plate boundaries occur in the Mediterranean – a subduction zone runs east from Sardinia, across the southern extremity of Italy along the southwestern coast of Greece and across the Aegean Sea towards Israel. Transform faults are also associated with the Anatolian and the Aegean microplates in the eastern Mediterranean region. The majority of tsunami sources in the Mediterranean are associated with these plate boundaries (Figure 1).

Current tsunami warning systems (TWSs) make use of seismographic recordings to detect the occurrence of earthquakes, volcanic eruptions, detonations of nuclear devices at sea, or underwater explosions (ITIC 2005). However, not all such events generate tsunamis. Given that unnecessary large-scale evacuations are costly and disruptive, it is necessary to confirm whether a potentially destructive tsunami has been generated by supplementing the seismic data with data on sea level changes at coastal tide gauge stations as well pressure fluctuations recorded on sensors on the sea floor.

Tsunami waves have long periods so that changes in hydrostatic pressure can be detected on the sea floor by an anchored seafloor bottom pressure recorder (or tsunameter) and a companion moored surface buoy for real-time communications (National Data Buoy Centre 2009). The surface buoy relays information between the tsunameter and a satellite network using an Iridium transceiver. The Iridium Satellite Network is a worldwide system capable of transmitting tsunami alerts throughout the Mediterranean quickly and efficiently. DART buoy data are then used to confirm the generation of a tsunami and to predict the tsunami hazard for locations where the waves will probably strike.

Coastal sea level gauges nearest the tsunami source are frequently destroyed by the waves. However, this action by itself is indicative that a destructive tsunami has been generated. Where coordination of information via a communication network component of a tsunami warning system exists, events at coastal sea-level monitoring stations can be used to provide warning to other coastal communities (Audet et al. 2008). Thus, the combination of coastal tide stations and DART buoys provide real-time sea level data that confirms tsunami generation and thus form the backbone of the detection component of tsunami warning systems.

3. MEASURING THE PERFORMANCE OF A TSUNAMI WARNING SYSTEM

The present paper examines the effectiveness of the current detection infrastructure (tsunami warning buoys and sea level monitoring stations) that may be employed as part of the proposed tsunami warning system for the coastal regions of the Mediterranean Sea. The measure of performance used in this analysis is the proportion of the coastal population that can receive a timely warning of the arrival of a tsunami, called the warning potential. This potential first appears in Braddock and Carmody (2001), where the concept was applied to the measurement of performance of an augmented tsunami warning system for the Pacific Ocean. Here, we modify their definition slightly to reflect the relative frequency of tsunamis generated.

In order to determine the warning potential for a particular tsunami, we must make a small number of time calculations. These include: a) the time taken by the tsunami to travel from the generation point to the population centre; b) the time taken by the tsunami to travel from the generation point to the nearest detector; and c) the time taken for the detection site to communicate with the warning centre and the population and a response to be undertaken. This latter time sum (b+c) must then be less than the tsunami travel time for a timely warning to be effectively issued. Populations potentially issued a timely warning are then summed and the proportion of the total population that could have been warned constructed (details follow). This is the warning potential.

To solve this problem, let the index set of detection sites (buoys and sea-level stations) be denoted w =1, … , W, where W describes the total number of detection sites. Let the index set for tsunami generation points (based on the historical record) be denoted by u =1, … , U, where U represents the total number of generation points. Let the index set for the population centres be v =1, … , V and P_v denote the population size. We use population size as a proxy for the number of people that may be affected by a tsunami as the actual population at risk depends on the height of the tsunami and the geography of the population centre. The time taken for the tsunami to travel to each population centre will be represented by $t_{u,v}$.

The first component in determining the time taken for a warning to reach a population centre is the time taken by the tsunami generated to reach a detection site. Let $t_{u,w}$ be this time. Let $t_{w,d}$ be the processing and transmission time to confirm the detection of a tsunami ($t_{w,d}$ will depend on whether the detector is a sea level station or a DART buoy). We define $t_w = t_{u,w} + t_{w,d}$ as the total time taken to issue a warning from the detection site at w for a tsunami generation point, u. The minimum value of t_w across all detection sites would then be the time taken to issue a tsunami warning for tsunami generation u. We denote this minimum time by t_w*. It follows that the population at v will be provided with a timely warning as long as t_w* + r_v < $t_{u,v}$, where r_v is the response time of the population at v.

The warning potential for a population centre v, for a tsunami generated at u is

$$p_{u,v} = \begin{cases} 0, & t_w^* + r_v \geq t_{u,v} \\ P_v, & t_w^* + r_v < t_{u,v} \end{cases} \quad (1)$$

That is, if timely warning is not received $p_{u,v}$ takes the value of 0, while if a population can receive a timely warning, the size of the population is taken. The warning potential for a given tsunami generation point is then calculated by summing the warning potentials for all population centres and standardising over the total population of all centres. That is, the warning potential for a generation point (P_u) is the proportion of the total population warned for a given tsunami generation point:

$$P_u = \left[\frac{\sum_{v=1}^{V} p_{u,v}(y)}{\sum_{v=1}^{V} P_v} \right] \quad (2)$$

We obtain a measure of the average performance of the TWS for all tsunami generation points by taking the average over the generation points or by summing the products of the relative frequency of tsunami generation and the warning potential over all generation points. The warning potential for each generation point and the average and weighted average warning potentials are thus dimensionless numbers between 0 (least preferable) and 1 (most preferable).

4. DATA

In order to solve this problem we will need data on existing stations and buoys, possible generation sites, and communication times.

4.1 Communication and response times

When changes in sea pressure reach the Bottom Pressure Recorder (BPR) of a DART buoy, the buoy can communicate data to tsunami warning centres in less than 3 minutes (Meinig et al 2005). Real-time sea level monitoring stations currently expect to transmit data within 6 minutes.

As different populations centres may require different response times, we consider a range of values for the population response time (though we use the same value of response time for each set of calculations) – 0 minutes, 15 minutes, 30 minutes, and 1 hour. These times were selected based on the minimum time it might take to move to an elevation above 10 meters, and the maximum time that could be utilized given the likely speeds of travel of a tsunami in the Mediterranean.

4.2 Tsunami wave speed, height and range

We compute tsunami travel times assuming an average wave speed. In the deep ocean, tsunami waves travel at speeds between 500 to 1000 km/hr (ITIC 2009). The wave speed of a tsunami may be approximated by $\sqrt{(9.8*\text{depth})}$. With a maximum depth in the Mediterranean of approximately 5150 metres, it follows that a tsunami wave may travel at approximately 225 metres per second, or approximately 800 km/hr (Nelson 2009). We examine a range of average speeds, from 200 km/hr to 800 km/hr, to accommodate variability in sea depth.

As previously mentioned, tsunami wave heights can vary widely. In order to estimate populations that may be affected by a tsunami, we considered only coastal populations below 100 metres and within 2 kilometres of the shoreline.

4.3 Population centres

One hundred and sixty-one population centres on the coast of the Mediterranean Sea were selected as potentially being affected by tsunami inundation. Without inundation maps and detailed geographical population data, we could not determine the exact figures for the population that may be affected by a tsunami. As a consequence, we used the population of the entire centre as a proxy for the population affected. Further, we decided to admit the possibility that any population centre could be affected by a tsunami generated at any of the points considered. This is unlikely as not all populations centres would be directly affected by tsunamis generated by some of the generation points considered (as, for example, a tsunami may only reach a centre following diffraction). We ignored this last point in calculating the travel times of tsunamis to population centres – the resulting times are then more than worse case scenarios of tsunami arrival.

The population centre data collected included the latitude and longitude, and population size. This data was based on the Gridded Population of the World from The Trustees of Columbia University in the City of New York. An initial filter was applied to this data to remove locations that were not a part of the countries surrounding the Mediterranean Sea. A second filter was manually applied to remove locations that were unlikely to be affected by a tsunami. The populations centres used can be found in Table A1 of the Appendix.

4.4 Locations of sea level stations and DART buoys

The location of sea level stations and DART buoys for the existing TWS can be found in the Global Sea Level Observing System (2009) and NOAA National Data Buoy Center (2009). The current full configuration of the TWS includes 2 tsunameter buoys and approximately 24 coastal sea-level stations (Table A2 and Figure 2). A further 4 candidate DART buoy locations were included later in the analysis to see if performance in the warning potential could be improved. These candidate locations were selected based on DART buoy bathymetric requirements (Spillane et al 2008) as well as whether they provided coverage of the region (with bathymetric data from the National Geophysical Data Center (2009a)). As far as possible, we selected potential DART buoy sites so as to avoid major shipping lanes and areas associated with piracy (National Geospatial Intelligence Agency 2009). Location information for the DART buoys sites and the sea-level stations are listed in Tables A2 of the Appendix and represented in Figure 2. A further 6 locations for real-time sea-level monitoring stations were also examined as part of an extended (and improved) TWS.

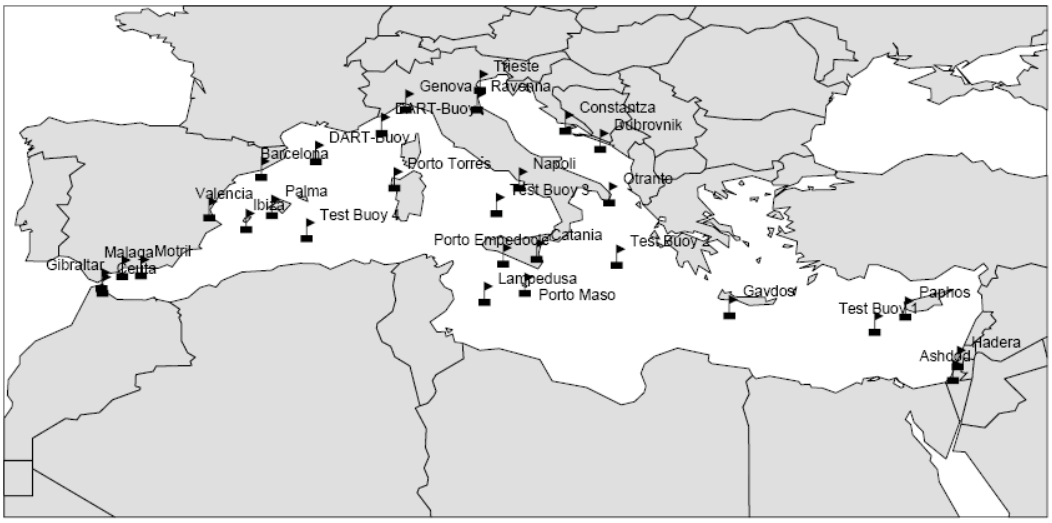

Figure 2 – Existing Sea level stations and existing and possible DART buoys sites

4.5 Potential tsunamigenic event locations

We based selection of tsunami generation points in the Mediterranean region on the historical record of magnitude and frequency of earthquakes and coastal volcanic activity available from the National Geophysical Data Center (2009) (Figure 1). The location of the tsunami generation points used in this study is a representative sample of these historical points. They are listed in Table A3 of the Appendix. With regard to the relative frequencies of tsunami events in the historical record, the Adriatic and Aegean Seas were approximately twenty-times more likely to generate a tsunami than the seas near Spain, France, Croatia, Egypt, Algeria, Israel, the Lebanon and Cyprus, while the seas surrounding southern Italy were approximately twice as likely to generate a tsunami.

5. SOLUTION APPROACH

We undertook the calculations of the times in Equation (1) and the warning potentials and average warning potentials (in Equations (2) and (3) respectively) using Excel spreadsheets. Workbooks were constructed for each of the tsunami wave speeds examined. Within each workbook, we constructed spreadsheets for undertaking the time calculations – generation point to detection site and generation site to population centre – with different response times. Travel times were determined using the Method of Great Circles (included as a cell formula). We then determined the time differences, and an "IF" statement was used to determine the $p_{u,v}$. The warning potentials for each generation point were then simply column sums divided by the sum of all populations, with the average warning potential, the average of these quotients. We then calculated the weighted average warning potentials also using the column sums. By undertaking the calculations in this fashion we were able to easily identify critical buoys and sea-level stations as well as identify regions requiring greater detector coverage.

6. RESULTS

6.1 The current configuration of sea-level stations and DART buoys

The table below shows the warning potentials for the TWS for each of the tsunami generation points when the estimated speed of the tsunami is 800 km/hr with the current detector configuration.

Table 1. Warning Potentials for a wave speed of 800 km/hr (reported to four significant figures)

Generation Point		*Nearest detector*	*Response Time*			
Location	*ID*		*0*	*15 min*	*30 min*	*1 hr*
Tyrrhenian Sea	1	23	0.9124	0.7025	0.5842	0.3984
Adriatic Sea	2	20	0.9917	0.8827	0.6439	0.3878
Algeria	3	5	0.9678	0.9266	0.8023	0.6645
Croatia	4	24	0.9937	0.8181	0.6969	0.4330
Cyprus	5	10	0.9964	0.9740	0.8291	0.6909
Egypt	6	25	0.9022	0.8327	0.7641	0.6461
France	7	29	0.9968	0.9968	0.8058	0.4536
Greece	8	14	0.8598	0.8200	0.7245	0.3169
Israel	9	10	0.9439	0.8623	0.8349	0.8179
Italy	10	19	0.9242	0.6745	0.6088	0.4262
Aegean Sea	11	20	0.8211	0.7382	0.5284	0.2378
Spain	12	3	0.9899	0.9467	0.9403	0.8086
Lebanon	13	13	0.9106	0.8607	0.8349	0.7693
Total average warning potential	-	-	0.9440	0.8539	0.7458	0.5444
Total weighted average warning potential	-	-	0.9139	0.8311	0.6872	0.4139

The following discussion should be considered recalling the qualification on the more than worst-case performance described previously (Section 4.3). From Table 1, we can see that the obvious result that increasing the population response time decreases the warning potential, in many cases substantially. For example, each 15 minutes of response time means that, for an estimated wave speed of 800 km/hr, the tsunami has travelled an additional 200 km. For near-shore tsunami events (and the historical record of tsunami generation points in the Mediterranean Sea are indeed near-shore), this has a significant impact on the proportion of the population that will be able to utilise the full response time. From Table 1 it can be seen that this is particularly true for tsunamis generated in and near the Adriatic Sea, while the warning potential is more robust for tsunamis generated near Algeria, Israel, Spain and Lebanon. This observation concerning the Adriatic Sea is of particular interest given the density of its coastal population and the fact that its bathymetry precludes locating DART buoys in much of its length. We are of the view that this suggests that sea-level monitoring stations on the coast of the Adriatic Sea play a crucial role in tsunami warning for the (coastal) population centres of the region. This result is reinforced when considering the differences between the average warning potentials and the weighted average warning potentials. The poorer performance on the weighted average potentials is a consequence of the poorer warning potentials of the Adriatic Sea, Greece, and Aegean Sea tsunami generation points. This also suggests that further sea level monitoring stations may be required on these coasts.

By examining the "Nearest detector" column in Table 1, it is clear that only one DART buoy (off the coast of France) is the nearest detector to a tsunami generation point. It may also be noted that sea-level station 10, at Paphos, plays a vital role in early warning as seen in its proximity to tsunami generation points in Cyprus and Israel. These results highlight the significant role played by coastal sea-level monitoring stations in the effectiveness of a TWS, as also found by Groen, Botten and Blazek (2010) in their study of the Indian Ocean tsunami warning detector system.

It should be obvious that a reduction in wave speed will result in an increase in warning potential. We will consider a response time of 30 minutes, and examine reductions in tsunami wave speed (though calculations have been done for all the response times described previously).

From Table 2, we can see that as speed increases, warning potentials decrease. Increasing the tsunami wave speeds for the Adriatic Sea and the Aegean Sea generation points (Points 2 and 4, and Point 11 respectively) yield more significant losses in warning potential (an average of 32.35% and 36.7% respectively) than for the other generation points (an average of 16.4%). We are again of the view that this result is a function of the relatively long and narrow shape of the Adriatic Sea and the relative lack of sea-level monitoring stations on the respective coasts.

For wave speeds of 200km/hr, 400km/hr and 600km/hr, best system performance in warning potential occurs for the tsunami generated near France, while best system performance for a wave speed of 800km/hr occurs for tsunamis generated by earth movements off the coast of Spain. This can be explained by the location of a DART buoy near the French tsunami generation point and the Spanish generation point being at an extreme of the Mediterranean.

Table 2. Warning Potentials for a response time of 30 minutes (reported to four significant figures)

Generation Point		*Wave Speed (km/hr)*			
Location	*ID*	*200*	*400*	*600*	*800*
Tyrrhenian Sea	1	0.8367	0.7775	0.6565	0.5842
Adriatic Sea	2	0.9899	0.8890	0.7361	0.6439
Algeria	3	0.9504	0.9266	0.8208	0.8023
Croatia	4	0.9920	0.8347	0.7193	0.6969
Cyprus	5	0.9913	0.9740	0.9111	0.8291
Egypt	6	0.9588	0.9022	0.8673	0.7641
France	7	0.9996	0.9968	0.9653	0.8058
Greece	8	0.8557	0.8254	0.8124	0.7245
Israel	9	0.9223	0.8924	0.8623	0.8349
Italy	10	0.8501	0.7601	0.6665	0.6088
Aegean Sea	11	0.8348	0.7414	0.6577	0.5284
Spain	12	0.9548	0.9515	0.9467	0.9403
Lebanon	13	0.9030	0.8648	0.8349	0.8349
Total average warning potential	-	0.9261	0.8720	0.8044	0.7458
Total weighted average warning potential	-	0.9461	0.8417	0.7653	0.6872

6.2 A possible expansion of the current configuration of sea-level stations and DART buoys

The current detector configuration was augmented by 4 DART buoys (Figure 2) using the criteria described in Section 4.4. It was found that one of the four additional buoys replaced an existing TWS detector – proposed DART buoy location (25) replaced a sea-level station (10) – as the nearest detector for the Egyptian tsunami generation point. For an estimated wave speed of 800km/hr, there was an 8.89% increase in warning potential for a 30-minute response time for that generation point. This increase amounts to approximately 5.25 million additional people across the coastal Mediterranean receiving a timely warning. Slightly smaller increases were observed for a one-hour response time (4.09% approx. or 2.41 million people approx.) and a 15-minute response time (7.76% approx. or 4.58 million people approx.). For slower tsunami wave speeds, the increase in performance of the TWS improved up to approximately 6% (for a tsunami wave speed of 200km/hr). Thus it can be seen that the addition of appropriately sighted DART buoys can have a significant impact on the warning potential of the Mediterranean TWS.

The relatively poor warning potentials for tsunamis generated in and near the Adriatic Sea suggest that further detectors on the coast of the Adriatic might improve average and weighted average warning potentials. It was also apparent that a real-time sea-level monitoring station(s) sited on the Turkish coast might also improve warning potentials. For this reason, we added six sites for coastal sea-level stations – two on the west coast of Turkey, one on the east coast of Greece, one on

the southern tip of Greece, and one on the west coast of Greece, with one on the coast of Albania. The following table shows the impact of these additions to the TWS on the warning potentials.

Table 3 includes the warning potentials as well as the change in warning potential from the current configuration of tsunami detectors (in brackets). From Table 3 we can see that while the improvement in total average warning potential is of the order of a few percent, significant gains in weighted average warning potentials and generation point-specific warning potentials are achieved. This confirms the previous suggestion that the deployment of real-time sea-level monitoring stations on the coasts of Greece and Turkey will improve the times available for populations responding to an impending tsunami.

Table 3. Updated Warning Potentials for a wave speed of 800 km/hr for additional stations
(Warning potentials reported to four significant figures)

Generation Point		*Nearest detector*	*Response Time*			
Location	*ID*		*0*	*15 min*	*30 min*	*1 hr*
Adriatic Sea	2	35 (20)	0.9950 (<1%)	0.8849 (<1%)	0.7132 (10.8%)	0.3962 (2.2%)
Greece	8	34 (14)	0.9439 (9.8%)	0.8384 (2.2%)	0.8135 (12.3%)	0.5103 (60.0%)
Aegean Sea	11	33 (20)	0.9910 (20.7%)	0.8900 (20.6%)	0.8211 (55.4%)	0.5583 (134.8%)
Total average warning potential	-	-	0.9625 (1.9%)	0.8671 (1.5%)	0.7782 (4.3%)	0.5846 (4.0%)
Total weighted average warning potential	-	-	0.9673 (5.8%)	0.8694 (4.6%)	0.7807 (13.6%)	0.5300 (28.1%)

7. CONCLUSIONS

In this study we examined the performance of the current available infrastructure of a Mediterranean TWS. This study utilized the historic record of tsunamis of the region, and the locations of existing sea level monitoring stations and DART buoys to conclude that, for short response times (15 minutes and 30 minutes) and a wave speed of 800 km/hr, the existing infrastructure will enable between 57% and 94% of the coastal populations of the Mediterranean to respond. For slower wave speeds, 600 km/hr for example, the performance improves, with the lower limit increasing to 65% for a 30-minute response time.

Performance at the regional level under the existing detection infrastructure is variable, with notably lower warning potentials associated with tsunamis generated in and near the Adriatic Sea. This is primarily a consequence of the geography and bathymetry of the sea, which prevents the effective deployment of DART buoys. This is exacerbated by the lack of real-time sea-level monitoring stations in Greece. In the coastal Adriatic then, more reliance must be placed on sea level monitoring, direct observation and seismic alerts. Poor warning potential is also noted for tsunamis

generated near the west coast of Italy. This is primarily a consequence of the fact that the tsunami generation points are close to the coast in this area and hence coastal populations in this region must rely more heavily on direct observation and seismic alerts to inform their response. If we consider the warning potentials for tsunamis generated in areas other than these, the lower limit of the warning potential increases to 72% of the coastal population (for a wave speed of 800 km/hr and response time of 30 minutes).

The performance of the Mediterranean TWS can be improved by the addition of a DART buoy at or near 34.07726N 30.96548E. Calculations suggest that the improvement in the number of people warned in the Mediterranean region could increase by as much as approximately 9% over the current TWS detector configuration. Further improvement can be achieved through the addition of three coastal sea-level monitoring stations. These results suggest that the existing infrastructure can provide an acceptable level of 15 or 30 minute warning but that improvement is possible. All results presuppose the coordination of real-time information from the countries bounding the rim of the Mediterranean Sea, and assume the historical record of tsunami generation is repeated into the future.

Acknowledgments

The authors wish to thank the Computational Research Support Unit, Science Faculty, University of Technology, Sydney for technical assistance with the construction of the map provided in Figure 2. The authors would also like to thank the editors for their contributions to the final paper.

REFERENCES

Amir L. and A. Cisternas, 2010, APPRAISAL OF THE 1790 ALBORAN TSUNAMI SOURCE IN THE WEST MEDITERRANEAN SEA AS INFERRED FROM NUMERICAL MODELLING: INSIGHTS FOR THE TSUNAMI HAZARD IN ALGERIA. Fourth International Tsunami Symposium of Tsunami Society International, 9th U.S. National and 10th Canadian Conference on Earthquake Engineering, July 25-29, 2010, Toronto, Ontario, Canada • Paper No. 1838.

Audet, C., G. Courtue, J. Dennis, M. Abramson, F. Gonzalez, V. Titov and M. Spillane (2008), Optimal Placement of Tsunami Buoys Using Mesh Adaptive Direct Searche, viewed 19 September 2009, <http://www.gerad.ca/Charles.Audet/Slides/Tsunami_JOPT.pdf >.

Braddock, R.D. and O. Carmody (2001), Optimal Location of deep-sea tsunami detectors, International Transactions in Operations Research, 8 249-258.

ESRI Australia, ArcGIS Version 9.3, <http://www.esriaustralia.com>.

Groen, L., L. C. Botten and K. Blazek (2010), Optimising the location of tsunami detection buoys and sea level detection sites in the Indian Ocean, International Journal of Operational Research, 4 (2) 174-188.

ICG/NEAMTWS-III (2007). Implementation Plan for the Tsunami Early Warning and Mitigation System in the North-Eastern Atlantic, the Mediterranean and Connected Seas (NEAMTWS), 2007–2011, UNESCO, viewed September 9 2009 <http://ioc3.unesco.org/ioc-24/documents/TS_73_NEAMTWSDraftImPlan.pdf>. IOC Technical Series No. 73 Action Plans. I.O.C.T. Series. Bonn, Germany.

International Tsunami Information Center (2005), "How we save lives", viewed 12 September 2009, <http://ioc3.unesco.org/itic/categories.php?category_no=140>.

International Tsunami Information Center, NOAA-UNESCO/IOC (2009), "Tsunami, Great Waves", viewed 12 September 2009, <http://ioc3.unesco.org/itic/files.php?action=viewfile&fid=808&fcat_id=137>.

MedGLOSS 2009, Last readings from MedGLOSS stations network , MedGLOSS, viewed 9 September 2009 <http://medgloss.ocean.org.il/map.asp>.

Meinig, C., S.E. Stalin, A.I. Nakamura, H.B. Milburn (2005), Real-Time Deep-Ocean Tsunami Measuring, Monitoring, and Reporting System: The NOAA DART II Description and Disclosure, viewed 12 September, available at <http://nctr.pmel.noaa.gov/Dart/dart_ref.html>.

National Data Buoy Centre, Deep-ocean Assessment and Reporting of Tsunamis (DART®) Description, viewed 14 December 2009, <http://www.ndbc.noaa.gov/dart/dart.shtml>.

National Geophysical Data Center NOAA 2009, Tsunami Events Full Search, sort by Date, Country, NOAA, viewed 12 September 2009 <http://www.ngdc.noaa.gov/nndc/struts/results?bt_0=&st_0=&type_8=EXACT&query_8=50&op_14=eq&v_14=&st_1=&bt_2=&st_2=&bt_1=&bt_10=&st_10=&ge_9=&le_9=&bt_3=&st_3=&type_19=EXACT&query_19=None+Selected&op_17=eq&v_17=&bt_20=&st_20=&bt_13=&st_13=&bt_16=&st_16=&bt_6=&st_6=&bt_11=&st_11=&d=7&t=101650&s=70>.

National Geophysical Data Center NOAA 2009a, NGDC/MGG - 2 minute bathymetry/topography image selector, NOAA, viewed 23 November 2009 <http://www.ngdc.noaa.gov/mgg/image/2minsurface/>.

National Geospatial-Intelligence Agency 2009, Anti-Shipping Activity Messages, National Geospatial-Intelligence Agency, viewed 9 September 2009 <http://www.nga.mil/portal/site/maritime/?epi_menuItemID=7c1695cead727e6e36890127d32020a0&epi_menuID=e106a3b5e50edce1fec24fd73927a759&epi_baseMenuID=e106a3b5e50edce1fec24fd73927a759>.

Nelson, S. 2009, Tsunami , Tulane University, viewed 9 September 2009 <http://www.tulane.edu/~sanelson/geol204/tsunami.htm>.

Pararas-Carayannis, G., 1973. The waves that destroyed the Minoan empire, Sea Frontiers 1972, 94-106.

Pararas-Carayannis, G.: 1974. The waves that destroyed the Minoan empire, Revised for Grolier Encyclopedia, Science Supplement, pp. 314-321.

Pararas-Carayannis, G., 1992. The Tsunami Generated from the Eruption of the Volcano of Santorin in the Bronze Age Natural Hazards 5:115-123,1992. 1992 Kluwer Academic Publishers (Netherlands.)

Pararas-Carayannis, G. 2006. The Potential for Tsunami Generation in the Eastern Mediterranean Basin and in the Aegean and Ionian Seas in Greece http://www.drgeorgepc.com/TsunamiPotentialGreece.html

Pararas-Carayannis G. & Mader, C.L. 2010. THE EARTHQUAKE AND TSUNAMI OF 365 A.D. IN THE EASTERN MEDITERRANEAN SEA, Fourth International Tsunami Symposium of Tsunami Society International, 9th U.S. National and 10th Canadian Conference on Earthquake Engineering, July 25-29, 2010, Toronto, Ontario, Canada • Paper No 1846

Pararas-Carayannis, G., Theilen-Willige, B. , & Helmut Wenzel, 2010. LOCAL SITE CONDITIONS INFLUENCING EARTHQUAKE INTENSITIES AND SECONDARY EFFECTS IN THE SEA OF MARMARA REGION - Application of Standardized Remote Sensing and GIS-Methods in Detecting Potentially Vulnerable Areas to Earthquakes, Tsunamis and Other Hazards, Fourth International Tsunami Symposium of Tsunami Society International, 9th U.S. National and 10th Canadian Conference on Earthquake Engineering, July 25-29, 2010, Toronto, Ontario, Canada • Paper No 1845

ScienceMaster 2009, ScienceMaster - Physical Science - Glossary of Earthquake Terms, ScienceMaster, viewed 12 September 2009 <http://www.sciencemaster.com/physical/item/earthquake_glossary.php#tsunami>.

The Belfast Telegraph 2009, Millions at risk from Mediterranean tsunami , The Independent, viewed 12 September 2009 <http://www.independent.co.uk/news/world/europe/millionsat-risk-from-mediterranean-tsunami-1712767.html>.

The Trustees of Columbia University in the City of New York 2009, Gridded Population of the World - GPW v3, CIESIN - Columbia University, viewed 9 September 2009 <http://sedac.ciesin.columbia.edu/gpw/global.jsp>.

Tsunami Institute 2009, Mediterranean, Tsunami Institute, viewed 12 September 2009 <http://www.tsunami-alarm-system.com/uploads/pics/tsunami_mediterranean.jpg>.

University of Cambridge 2009, Tsunami risk in the Mediterranean, University of Cambridge, viewed 12 September 2009 <http://www.researchhorizons.cam.ac.uk/researchnews/tsunami-risk-in-the-mediterranean.aspx>.

Westall, S. 2008, "Mediterranean tsunami warning system set for 2011." Viewed 12 September 2009, <http://www.reuters.com/article/idUSL1685238820080416>.

APPENDIX

Distance calculation

The calculation of the following distances is based on the Method of Great Circles. The Method of Great Circles calculates spherical distances from pairs of latitude and longitude values using the shortest. A great circle is a circle defined by the intersection of the surface of the Earth and any plane that passes through the centre of the Earth. The great circle (geodesic) distance between two points, P_1 and P_2, located at latitude x_1 and longitude x_2 of (x_{11},x_{21}) and (x_{12},x_{22}) on a sphere of radius a is

$d = a \cos^{-1} \cos x_{11} \cos x_{12} \cos (x_{21} - x_{22}) + \sin x_{11} \sin x_{12}$

Here a is the radius of the Earth (assuming it is spherical).

Input Data

Table A1 – Population Centres

Population Centre	*Lat. (N)*	*Long. (E)*	*Pop^n*	*Population Centre*	*Lat. (N)*	*Long. (E)*	*Pop^n*
Israel				*Turkey*			
Khefa	32.59875	34.9531	416500	Hatay Province	36.51361	36.205	1386224
Ha Merkaz	32.09817	34.89002	1200800	Icel	36.53417	33.93917	989635
Telaviv	32.07477	34.81803	1136900	Mugla	36.90381	28.6319	185175
Hadaron	31.6125	34.65417	69100	Aydin	37.76917	27.53667	313041
Cyprus				Izmir	38.47627	27.18134	2682948
Ammochostos District	35.03333	33.92738	32090	Canakkale	40.07556	26.72333	171578
Larnaka District	34.93776	33.56823	92857	*Syria*			
Lefkosia District	35.09171	33.27422	210808	Tartus	34.9	35.9	52589
Lemesos District	34.72279	33.00172	168360	Ladhaqiyah	34.66556	35.84778	365968
Pafos District	34.80357	32.42976	43121	*Serbia and Montenegro*			
Greece				Montenegro	41.92972	19.20806	13145
Dodekanisos	36.55781	27.60813	156609	*Lebanon*			
Samos	37.72778	26.79556	23100	Albiqa	33.92394	36.0735	136600
Lesvos	39.225	26.233	61300	Assamal	34.34	35.77	210000
Hios	38.37761	26.11381	33879	Jabal Lubnan	33.93771	35.60264	173100
Lasithi	35.13565	25.79076	40700	Annabatiyah	33.385	35.525	98900
Rodopi	41.08769	25.47846	64486	Bayrut	33.87194	35.50972	1100000
Kiklades	37.01963	25.21273	53300	Aljanub	33.46963	35.40037	261600
Iraklion	35.21731	25.14731	202212	*Egypt*			
Xanthi	41.14	24.89643	65618	Sina Ash Shamaliyah	31.20389	34.01694	125147
Rethimni	35.29429	24.68429	38887	Bur Said	31.26667	32.3	469533
Kavala	40.89808	24.45654	113002	Dumyat	31.35889	31.7325	236716
Hania	35.47765	23.94569	97073	Al Garbiyah	30.88397	31.03329	1029842

Population Centre	*Lat. (N)*	*Long. (E)*	*Pop^{n}*	*Population Centre*	*Lat. (N)*	*Long. (E)*	*Pop^{n}*
Attiki	37.99476	23.7429	3729385	Kafr Ash Shaykh	31.23377	30.86065	495804
Evvoia	38.53778	23.68694	143384	Matruh	31.19	27.83667	73547
Halkidiki	40.27203	23.49553	71900	*Slovenia*			
Magnisia	39.28375	23.05	168139	Divaca	45.68778	13.97167	3829
Thessaloniki	40.64427	22.99854	1020945	Komen	45.81361	13.74667	3515
Argolis	37.54721	22.9325	71700	Obalnokraska	45.57874	13.71046	90688
Fthiotis	38.71469	22.8825	44600	*France*			
Korinthia	37.94898	22.8143	98487	Saint Maxime	43.3167	6.65	15565
Lakonia	36.83533	22.726	42200	Saint Tropez	43.26667	6.633333	8154
Larisa	39.74857	22.62	13100	Languedoc-Roussillon	43.19167	2.852083	647714
Pieria	40.28214	22.56064	88109	Corsedusud	42.30972	9.091667	153726
Imathia	40.61	22.536	8500	*Croatia*			
Arkadia	37.43286	22.50571	39800	Sibenikknin	43.87787	16.08713	51460
Messinia	37.07737	21.87368	95350	Zadarknin	44.04324	15.33139	78756
Ilia	37.74483	21.44241	97400	Likasenj	44.80167	15.17269	15988
Arta	39.1575	20.93375	27900	Primorjegorskikotar	45.17685	14.51639	183900
Aitoliakaiakarnania	38.91333	20.89833	11400	Istra	45.14208	13.73438	104780
Zakinthos	37.77	20.84333	17700	Dubrovnik Neretva	42.83685	17.53324	62036
Levkas	38.83	20.7	6900	Split Dalmacija	43.48668	16.57762	279990
Preveza	39.17714	20.69714	30400	*Tunisia*			
Kefallinia	38.245	20.57	15600	Halqalwadi	36.85	10.32	61600
Thesportia	39.5	20.32429	18800	Bardo	36.82	10.13	65669
Kerkira	39.58397	19.90304	50400	Mahdia	35.36556	10.97299	95115
Tripoli	32.8925	13.18	1250000	Monastir	35.67154	10.83436	273089
Albania				Sfax	34.72167	10.76301	355148
Sarande	39.88	20	14548	Nabeul	36.65171	10.74212	315584
Kruje	41.52333	19.73	36653	Sousse	35.82561	10.57761	249692
Lushnje	40.95	19.71	38341	Tunis	36.83875	10.28875	809908
Kurbin	41.64	19.71	23508	Benarous	36.73056	10.25611	238613
Lezhe	41.79	19.65	16670	Manouba	36.80778	10.10111	21799
Fier	40.69889	19.64778	82700	Gabes	33.84083	10.0625	72630
Vlore	40.51	19.57	92089	Ariana	36.87311	10.04172	231565
Kavaje	41.2	19.56	28269	Bizerte	37.18597	9.879722	255882
Durres	41.25333	19.55667	132338	Jendouba	36.62889	8.737153	88200

Population Centre	*Lat. (N)*	*Long. (E)*	*Pop^n*	*Population Centre*	*Lat. (N)*	*Long. (E)*	*Pop^n*
Shkoder	42.07	19.51	86122	*Algeria*			
Malsiemadhe	42.2	19.43	4080	Tarf	36.88333	8.483333	21254
Libya				Annaba	36.86667	7.8	352523
Bardiyah	31.75	25.07	7500	Skikda	36.88333	6.888889	210649
Tubruq	32.08361	23.97639	92000	Jijel	36.65333	5.902222	196813
Darnah	32.765	22.63917	73000	Bejaia	36.60833	4.816667	177196
Sahhat	32.83	21.86	28100	Tiziouzou	36.70167	4.066667	140407
Albayda	32.76639	21.74167	74500	Boumerdes	36.73333	3.538889	106543
Almarj	32.5	20.83333	97000	Alger	36.74167	3.219167	218024
Alcquriyah	32.53	20.57	15500	Chlef	36.31667	1.308333	202504
Suluq	31.67111	20.25111	10400	Mostaganem	35.91667	0.1	125911
Azzwaytinah	30.95	20.12	12200	Oran	35.75	-0.53333	730530
Bangaz	32.12	20.07	500000	Aintemouchent	35.18333	-1.25	92557
Marsaalburayqah	30.41667	19.57861	8000	Tlemcen	35.05833	-1.575	46723
Surt	31.20611	16.59472	38500	*Spain*			
Misratah	32.37833	15.09056	135000	Girona	42.00179	2.862564	304896
Zeleiten	32.46667	14.56667	26000	Balears	39.55938	2.789583	647458
Zitan	32.48	14.56	100000	Baleares	39.56667	2.65	333801
Alhums	32.66	14.26	120000	Cataluna	41.5	2.216667	160262
Azzwiyah	32.76	12.72	116000	Barcelona	41.49908	2.138495	4223710
Sabratah	32.79194	12.48472	46500	Tarragona	41.00417	1.036111	371368
Italy				Castello	40.32333	0.31	55113
Calabria	39.0237	16.27778	1082147	Alacant	38.75763	0.105009	79542
Campania	40.8436	14.47082	4467955	Murcia	37.41	-1.59	27771
Palermo, Sicilia	38.11667	13.36668	657935	Almeria	36.97939	-2.4797	387701
Abruzzo	42.44322	14.02897	738754	Melilla	35.3	-2.95	66411
Marche	43.38017	13.39274	962202	Malaga	36.71368	-4.56579	1121504
Lazio	41.78436	12.82868	4378693	Ceuta	35.9	-5.29	71505
Puglia	40.76781	17.15583	3491037	*Morocco*			
Calgliari, Sardegna	39.24639	9.0575	400000	Oriental	35.17	-2.95	112450
Porto Torres, Sardegna	40.83333	8.4	22217	Tazaalhoceimat aounate	35.19958	-3.89972	80716
Bosnia and Herzegovina							
Serb Republic	42.71	18.34	28500				

Table A2 – Locations of Detectors

Existing Real-time Sea-level Stations							
Location	*ID*	*Latitude*	*Longitude*	*Location*	*ID*	*Latitude*	*Longitude*
Gibraltar	1	36.117	-5.35	Hadera	13	32.47053	34.86306
Malaga	2	36.7	-4.4	Gavdos	14	34.848	24.119
Motril	3	36.716	-3.516	Trieste	15	45.42268	12.4235
Valencia	4	39.45	-0.31	Ravenna	16	44.49645	12.27978
Ibiza	5	38.9	1.43	Genova	17	44.49645	8.92568
Barcelona	6	41.35	2.15	Porto Empedocle	18	37.29016	13.52432
Ceuta	7	35.9	-5.317	Napoli	19	40.83962	14.26913
Palma	8	39.55	2.63	Otranto	20	40.14617	18.49672
Porto Maso	9	35.909	14.519	Porto Torres	21	40.84071	8.40437
Paphos	10	34.78333	32.401	Lampedusa	22	35.48333	12.61667
Constantza	11	43.507	16.442	Catania	23	37.49699	15.09344
Ashdod	12	31.811	34.635	Dubrovnik	24	42.65	18.06667
DART Buoys							
Test Buoy 1	25	34.07726	30.96548	Test Buoy 4	28	38.46404	4.281104
Test Buoy 2	26	37.2073	18.83862	DART-Buoy	29	43.4	7.8
Test Buoy 3	27	39.63586	13.19198	DART-Buoy	30	42.103	4.703
Proposed Real-time Sea-level Stations							
Test SlS 1 (near Mugla)	31	36.56256	28.01476	Test SlS 4 (Laconia)	34	36.80529	22.62476
Test SlS 2 (east of Lesvos)	32	39.07627	26.09159	Test SlS 5 (west of Kerkira)	35	39.59183	19.80302
Test SlS 3 (east of Larissa)	33	39.57667	22.93225	Test SlS 6 (vicinity of Lezhe)	36	41.82766	19.5448

Table A3 – Tsunami Generation Points

Location	*ID*	*Latitude*	*Longitude*	*Location*	*ID*	*Latitude*	*Longitude*
Tyrrhenian Sea	1	38.6929	15.259	Greece	8	37.222	23.756
Adriatic Sea	2	39.934	19.371	Israel	9	33.805	32.9125
Algeria	3	36.754	1.554	Italy	10	40.67053	13.78057
Croatia	4	42.445	17.326	Aegean Sea	11	39.4	22.3
Cyprus	5	34.8	32	Spain	12	36.44433	-2.589
Egypt	6	31.901	30.582	Lebanon	13	33.624	34.992
France	7	43.04	6.937				